Noise factor of MZPI radar

Hudson, A.C.

https://doi.org/10.4224/21272336

ERA - 186

SECRET

NATIONAL RESEARCH COUNCIL OF CANADA

RADIO AND ELECTRICAL ENGINEERING DIVISION

NOISE FACTOR OF MZPI RADAR

A. C. HUDSON

OTTAWA

JULY 1950

ERA-186

SECRET

National Research Council of Canada

Radio and Electrical Engineering Division

NOISE FACTOR OF MZPI RADAR

A.C. Hudson

Introduction	-	3
Text	-	18
Figures	-	27

ABSTRACT

Noise factors of the Canadian MZPI and the British Admiralty Type 980 Radar Receiver have been measured using both the signal-generator and fluorescent-lamp methods. An improved preamplifier for the MZPI which lowers the over-all noise factor from approximately 14.0 to 10.4 decibels is described. Possible future improvements to the MZPI are suggested.

CONTENTS

NOISE FACTOR OF MZPI RADAR

1. Introduction

The noise factor of the MZPI (A.A. No. 4, Mk.VI) radar has been compared with that of a similar radar of more recent design. As a result of this investigation, certain modifications to improve the noise factor are recommended. The work was carried out concurrently with a number of other projects during the period February, 1948, to June, 1950, and will be discussed in the order in which it was done.

2. British Receiver

The British Admiralty have kindly lent a Type 980 Receiver for this investigation(1). This equipment employs the Dahl mixer(2),(3) and is stated to have a noise factor of about 10 decibels under field conditions.

3. Comparison of MZPI and Type 980 Receiver Design

A brief comparison of the two receivers from the point of view of this report follows:

	MZPI	Type 980
Operating frequency	S-band	S-band
Intermediate frequency	30 mc	13.5 mc.
Local Oscillator	reflex klystron 707B	Heil tube CV-230
Mixer	co-axial	waveguide (Dahl)
T/R	721 A/B	CV-293
Pre-T/R	none	CV-294
Anti-T/R	none	CV-294
Pre-amplifier (first tube)	6AC7 pentode	VR-136
Bandwidth	1.5 mc.	4, 1.5, 0.5 mc.
Crystal	1N21B	CV-364

The low intermediate frequency is used on the Type 980 Receiver in order to obtain a low intermediate-frequency noise factor. In general, any reduction in intermediate frequency will result in increased local oscillator noise and in less discrimination against interference at the image frequency; in some cases, however, the improvement in intermediate-frequency noise factor will outweigh these considerations.

4. Definition of Noise Factor

The noise factor of a linear receiver and antenna combination is defined as: the ratio of the noise power delivered to a load at the output of the intermediate-frequency amplifier, to that power which would be delivered if there were no sources of noise in the receiver. For a superheterodyne receiver having appreciable image response this ratio must be multiplied by an image correction factor defined by:

$$n = \frac{\int_{o}^{\infty} g \, df}{\int_{a}^{b} g \, df} \qquad \text{Eq. (1)}$$

"g(f)" is the power gain of the receiver as a function of frequency, and "a" and "b" are limits which define the useful channel as distinct from the image or any other spurious responses. The image correction is discussed further in Appendix I.

5. Noise Factor Measurements — Signal Generator Method

The first method used to measure the noise factor was to feed radio-frequency power from a signal generator to the antenna terminals of the radar receiver, and adjust the level until the power level at the input to the second detector was double that due to receiver noise alone. If the noise bandwidth of the receiver is known, the over-all noise figure can be calculated from the signal power level by means of the following equation (see Appendix I):

$$F = \frac{S_I}{K \, T_o B_o} \qquad \text{Eq. (2)}$$

where, F = noise factor as a power ratio

S_I = available excess power from the signal generator in watts

K = Boltzman's constant = 1.38×10^{-23} Joules/°K

T_o = absolute room temperature in °K (assumed to be 292°K)

B_o = noise bandwidth of the receiver in c.p.s.[4]

A block diagram of the measuring apparatus is given in Fig.1.

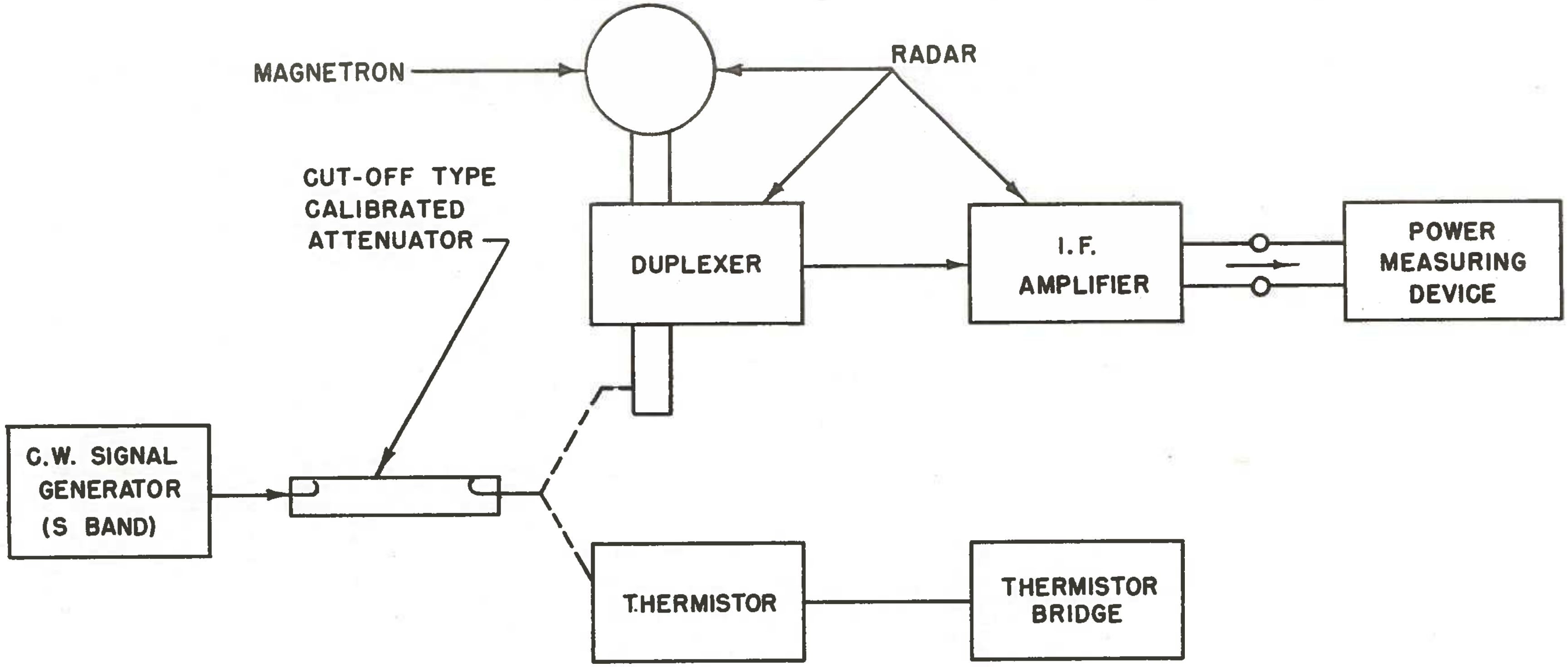

FIG. I – MEASUREMENT OF NOISE FACTOR BY SIGNAL GENERATOR METHOD

SECRET

Two standard signal generators were used alternately — a Browning Type TGS-3BL, and a Hewlett-Packard Type 616A. The Hewlett-Packard power calibration was found to agree within one decibel with the calibration made here, which was obtained using a thermistor bridge, Type TBN-3EV. The Browning signal generator was found to be considerably in error, and the instrument was recalibrated.

Thermistor bridge measurements cannot be made accurately below about 20 decibels below 1 milliwatt, while the signal generator must be used at about 100 decibels below 1 milliwatt. Thus, the attenuator in the signal generator must be assumed correct over a range of 80 decibels. This assumption constitutes the most serious source of error in this method. The error was minimized by comparing various attenuators with one another in steps, using the substitution method.

The signal generator was connected to the antenna wave guide by means of a calibrated length of lossy cable, and a matched coaxial-to-wave-guide transformer. For the Type 980 Receiver, a tapered section from Canadian to English wave guide was also necessary.

It is very difficult to obtain accurate results by this method, and it has been superseded by the plasma oscillation (fluorescent lamp) method described in Section 14.

6. Receiver Tuning

When using the Type 980 Receiver it was necessary to tune the local oscillator, the T/R cavity, and the anti-T/R cavity. The MZPI has no anti-T/R cell. On the latter receiver, therefore, it was necessary to install a typical magnetron of known operating frequency, and to perform the noise measurement at this frequency. A small error in match was introduced because the magnetron was not at operating temperature.

7. Intermediate-Frequency Power Measurements

The theory of the response of an ideal diode in the presence of a sine-wave signal plus random noise was published in 1944[5]. It was hoped at first that the diode second detector would approximate an ideal diode well enough to use the second detector as a power measuring device. However, an error of 1.2 decibels* resulted when using this method. It was found necessary to replace the second detector with a germanium crystal, and to operate at a second detector current of less than 10 microamperes. A spotlight

*This error was evaluated by comparison with the germanium crystal method.

galvanometer, type 2420D, was used to measure this current. In this region the d-c crystal current can be assumed to be proportional to the square of incident alternating voltage, and sine-wave power and random noise power will add linearly.

8. Results

Figs. 2 and 3 give a comparison of the noise factor of the Type 980 and the MZPI receivers. Each block represents the average of ten or more noise factor determinations on a single crystal.

The difficulties of the method are illustrated by the spread in readings on one crystal (See Fig.4).

9. Expected Noise Factor

The expected noise factor has been calculated from typical crystal constants.

The following equation applies:

Radar noise factor in decibels $= D + T + g + 10 \log_{10} (F + t - 1 + \Delta t)$, Eq. (3)

where D = duplexer mismatch in decibels
T = T/R loss in decibels
g = crystal conversion loss in decibels
F = intermediate-frequency noise factor as a power ratio
t = excess noise temperature ratio of crystal
Δt = apparent increase in excess noise temperature due to local oscillator noise.

As a first approximation we may assume that $D + T = 1$ decibel, and that Δt is negligible.

The value of F (intermediate-frequency noise factor) was expected to be about 4.5 decibels, this being about the best figure obtainable using a pentode-connected 6AC7 as the input tube. Actual measurements on preamplifier Serial 306 indicated a noise factor of 5.5 decibels (see histogram Fig.5); that is, a power ratio of 3.55.

Typical values of "g" and "t" for 1N21B crystals are indicated in Figs. 6 to 9. The histograms (Figs. 6 and 8) represent data published by M.I.T.(6), while Figs. 7 and 9 show measurements made at N.R.C.*

From these data typical 1N21B crystals can be selected and the expected noise factor calculated using Eq. (3). This calculation is outlined in Table I.

* These measurements were made by W.J. Medd of the Solar Noise Group.

NOISE FACTOR, USING SIGNAL GENERATOR METHOD

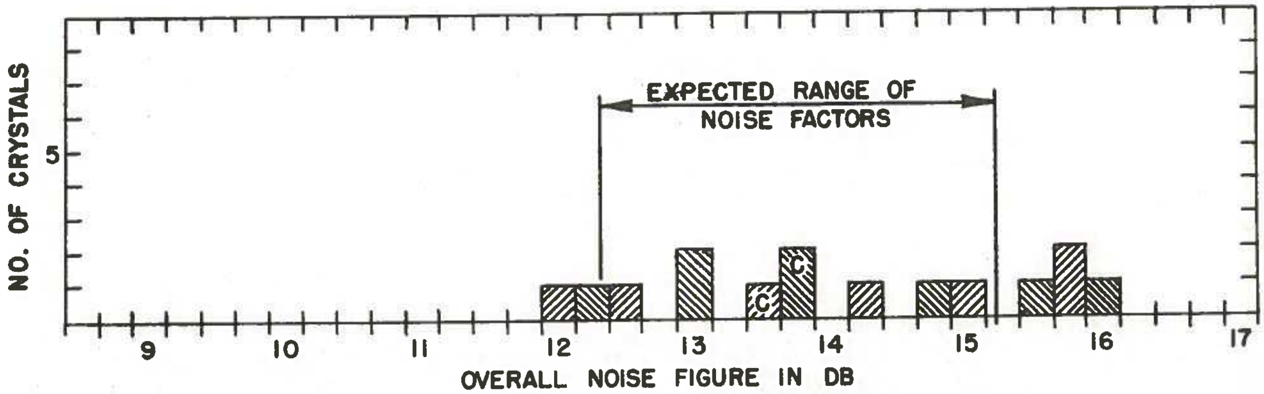

FIG. 2 — MZPI RECEIVER (VARIOUS IN21B AND IN21C CRYSTALS)
(IN21C ARE MARKED "C")

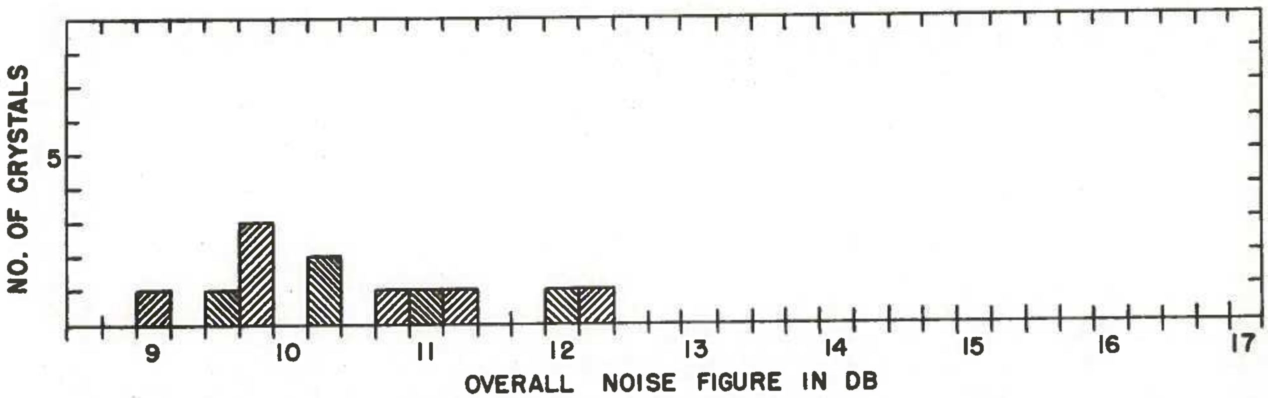

FIG. 3 — 980 RECEIVER (VARIOUS CV364 CRYSTALS)

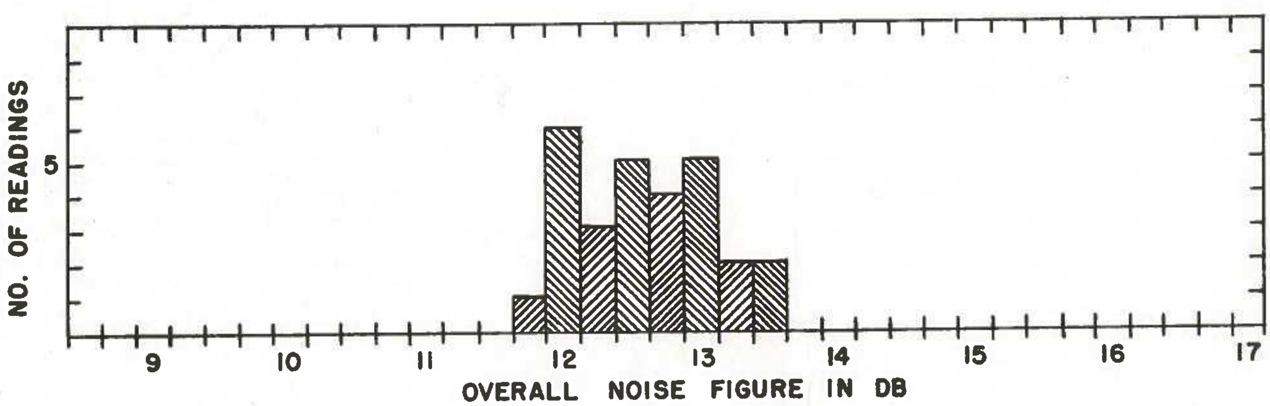

FIG. 4 — TYPICAL VARIATIONS WITH TIME IN READING ON SAME CRYSTAL

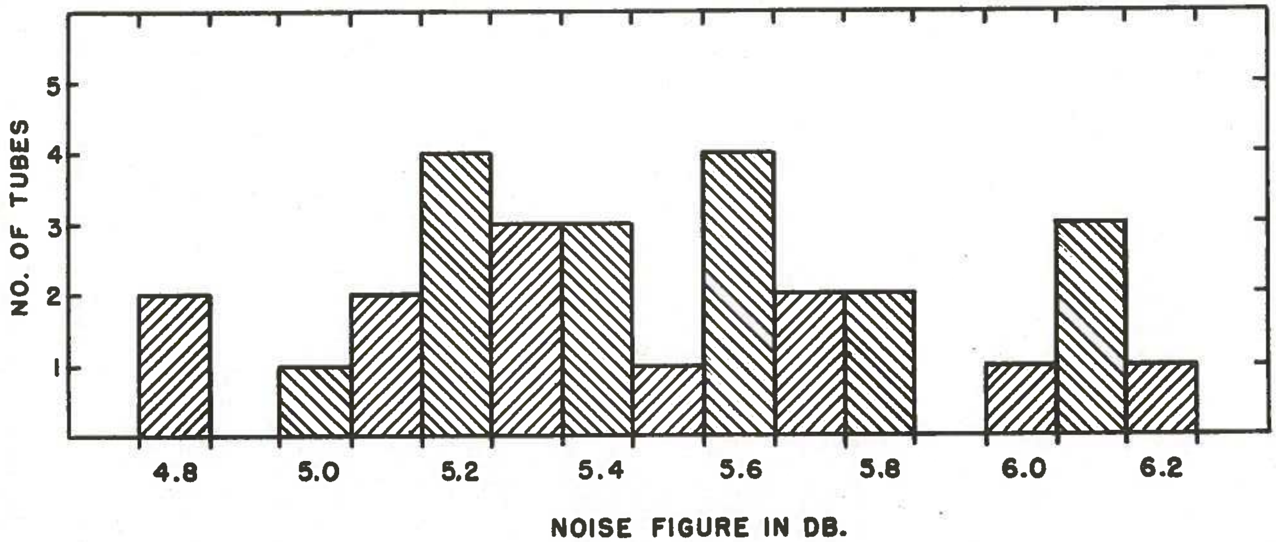

FIG. 5 – MZPI PREAMPLIFIER SERIAL 306 (VARIOUS 6AC7'S IN FIRST STAGE)

SECRET

CONVERSION LOSS (g) OF S BAND CRYSTALS

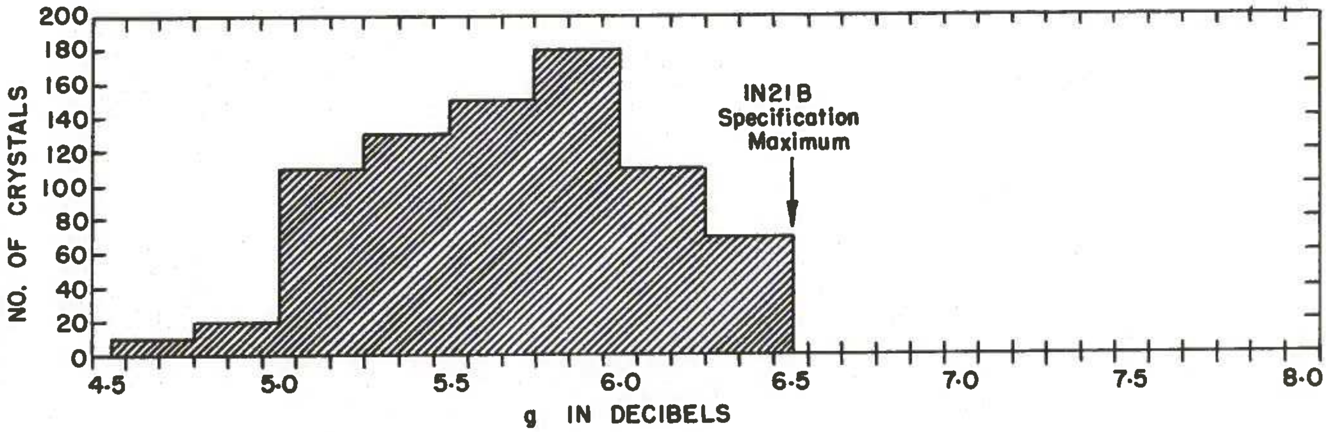

FIG.6—M.I.T. PUBLISHED VALUES FOR IN21B CRYSTALS
(REF. (6) PAGE 32)

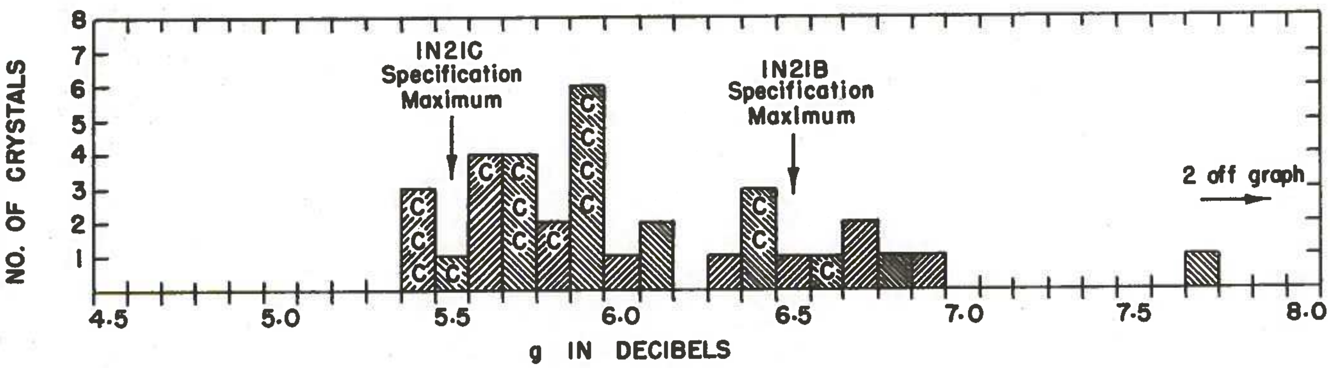

FIG.7—N.R.C. MEASURED VALUES FOR IN21B AND IN21C CRYSTALS
(IN21C ARE MARKED "C")

NOISE TEMPERATURE RATIO (t) OF S BAND CRYSTALS

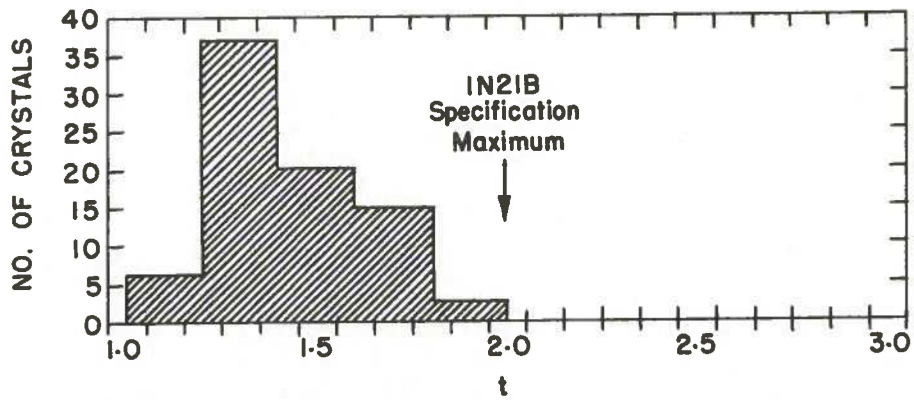

FIG. 8 — M.I.T. PUBLISHED VALUES FOR IN21B CRYSTALS

(REF. (6) PAGE 32)

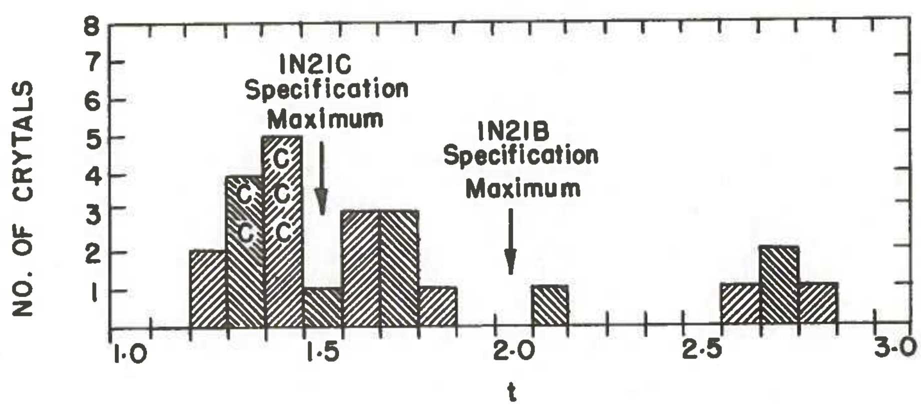

FIG. 9 — N.R.C. MEASURED VALUES FOR IN21B AND IN21C CRYSTALS (IN21C ARE MARKED "C")

TABLE I

	M.I.T. Published Data		N.R.C. Measurements	
	good crystal	poor crystal	good crystal	poor crystal
g	5.0 db	6.5 db	5.6 db	6.9 db
t	1.1	1.9	1.2	2.8
F (= 3.55) + t - 1	3.65	4.45	3.75	5.35
$10 \log_{10}(F + t - 1)$	5.6 db	6.5 db	5.7 db	7.3 db
(D + T) + g	6.0 db	7.5 db	6.6 db	7.9 db
Noise Factor (db.)	11.6	14.0	12.3	15.2

Using the assumptions previously mentioned — that the duplexer mismatch plus the T/R loss is about one decibel, and the local oscillator noise is negligible — Table I indicates the expected range of MZPI noise factor with various type 1N21B crystals.

This range is 11.6 to 14 decibels using the M.I.T. values of crystal constants, or 12.3 to 15.2 decibels based on values measured at N.R.C. This latter range has been indicated on Fig. 2, and is seen to be substantially in agreement for the best crystals with measured values using the signal generator method, and the fluorescent lamp method to be described later (See Fig.17).

This agreement suggests that the assumed values for D, T and t are approximately correct, and also that little improvement in noise factor could be expected by alterations in the mixer.

10. Possible Methods of Improving the Noise Factor

To reduce the noise factor, "g" and "t" can be improved only by selecting crystals, or possibly by undertaking an extensive program of crystal research. D and T possibly could be reduced; however, the agreement between measured and expected noise factors for the best crystals suggests that the quantity (D + T) is of the order of one decibel, and thus any improvement here would not be large.

Current practice permits intermediate-frequency noise figures of between 1.5 and 2 decibels. Re-calculation of Table I using an intermediate-frequency noise figure of 1.75 decibels gives the following theoretical noise factors:

TABLE II

	Crystal Constants according to:	
	M.I.T.	N.R.C.
good crystal	8.04 db	8.9 db
poor crystal	11.3 db	13.1 db

It was decided that the most promising approach would be to redesign the intermediate-frequency preamplifier, and to defer consideration of other changes.

11.. Cascode Preamplifier

A four-stage preamplifier was built, using the cascode input circuit with a triode-connected 6AK5 as the first tube. The schematic diagram for this preamplifier is given in Fig.10. Single tuned circuits were employed for simplicity, since the required bandwidth is only 1.5 megacycles. A noise factor of 1.7 decibels was obtained (see histogram Fig.11). Various input circuits were tried in addition to the one shown in Fig. 10. These included a degenerate π-section, and an optimum network as designed by the method outlined by Lebenbaum(7).

After adjustment, each of these circuits yielded a noise factor of 1.7 decibels, which suggests that this is the best obtainable with 6AK5's in a cascode circuit at 30 megacycles. Wallman, however, quotes a median of 1.35 decibels; the measurements being made on one hundred 6AK5's(8).

The following methods were tried without success in an effort to reduce further the noise factor of the intermediate-frequency preamplifier:

(1) Operation of the first stages at reduced filament voltage.

(2) Substitution of a Western Electric Type 404A tube in the first stage, with a corresponding circuit adjustment.

(3) Substitution of various 6J6's in the grounded-grid stage.

(4) Improvements in the second 6AK5 stage.

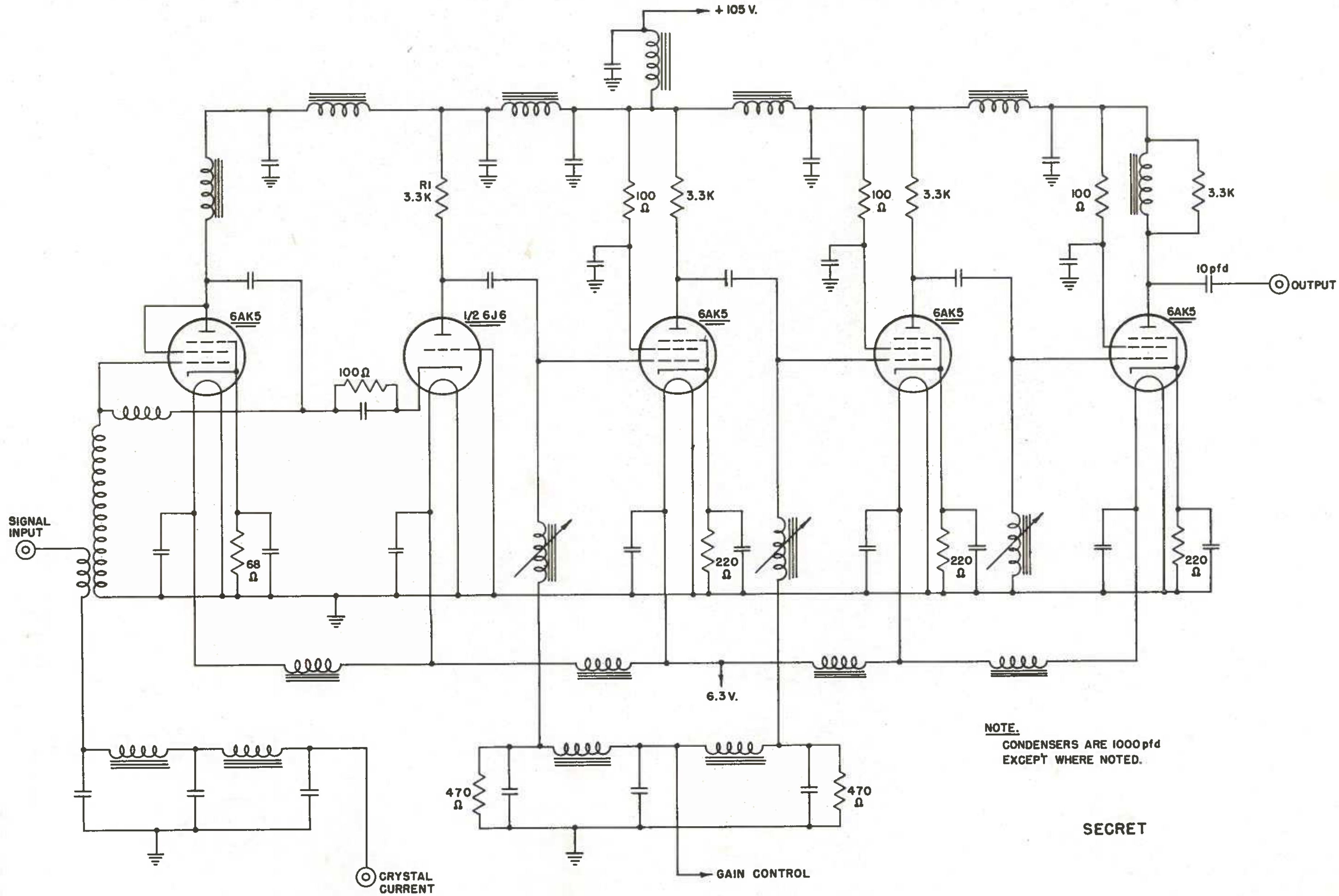

SECRET

FIG. 10 – CASCODE PREAMPLIFIER SCHEMATIC

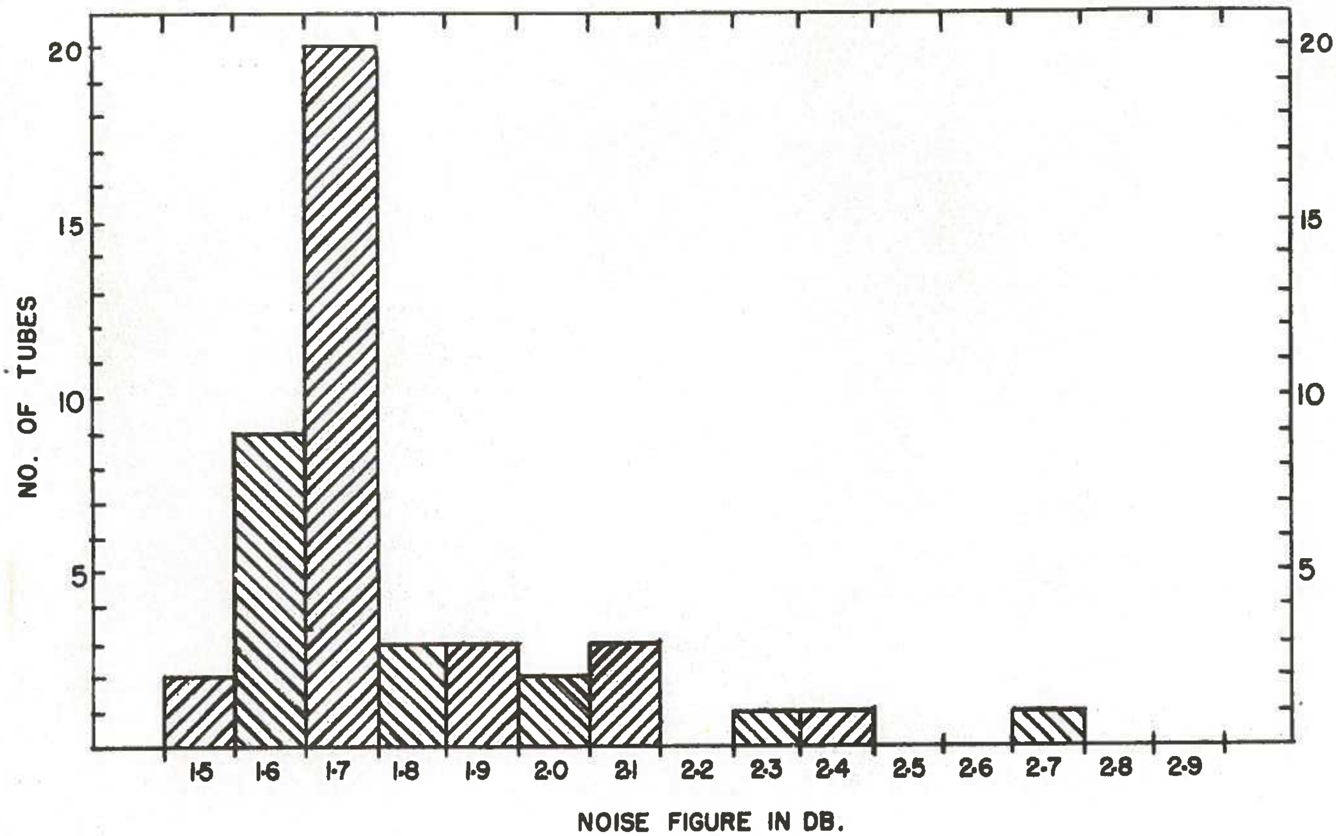

FIG. 11 — CASCODE PREAMPLIFIER (VARIOUS 6AK5'S IN FIRST STAGE)

(5) Reduction of resistor noise in R_1.

(6) Substitution of a type 6J4 tube in the grounded-grid stage.

Figs. 12 and 13 are two views of the experimental model of this preamplifier. Its use resulted in the expected improvement in over-all noise factor. This is discussed in Section 16.

12. Intermediate-Frequency Noise Factor Measuring Method

Measurements of intermediate-frequency noise factor were carried out using conventional technique(9) and need not be discussed in detail. It should be noted, however, that some RCA Type-5722 noise diodes were found to give excessively high readings. It appeared that some of the plate current was space-charge-limited, which could possibly be due to an offset filament. Sylvania Type X6030 and Marconi Osram Valve Co. Type CV-172 diodes were satisfactory.

13. Fluorescent Lamp Noise Source

The work had reached the stage described above late in 1949. At this time Mumford(10) reported that a commercial fluorescent lamp mounted in a wave guide comprised a satisfactory microwave noise source. A noise source using this technique was constructed. The lamp was mounted diagonally between the wide faces of the guide to improve the match. Fig.14 is a photograph of this mount. It is interesting to note that within five months of the publication of Mumford's results noise sources of this type were available commercially to cover a frequency range from 2,600 to 12,400 megacycles*. The diagonal mounting is also used in the commercial models.

Calibration of the noise source against a heat load was made with the co-operation of the Solar Noise Group, of this Division of N.R.C.

A block diagram of the calibrating equipment is shown in Fig. 15. For noise factor measurements the effective temperature of the lamp is most conveniently expressed by the excess noise power ratio in decibels.

$$E = \text{excess noise power ratio in db} = 10 \log_{10}\left(\frac{T}{T_o} - 1\right),$$

where T_o = 292°K ($\doteqdot$ room temperature),

and T = equivalent noise temperature of the lamp.

* Kay Electric Company, Pine Brook, N.J., U.S.A. "Microwave Mega-Nodes".

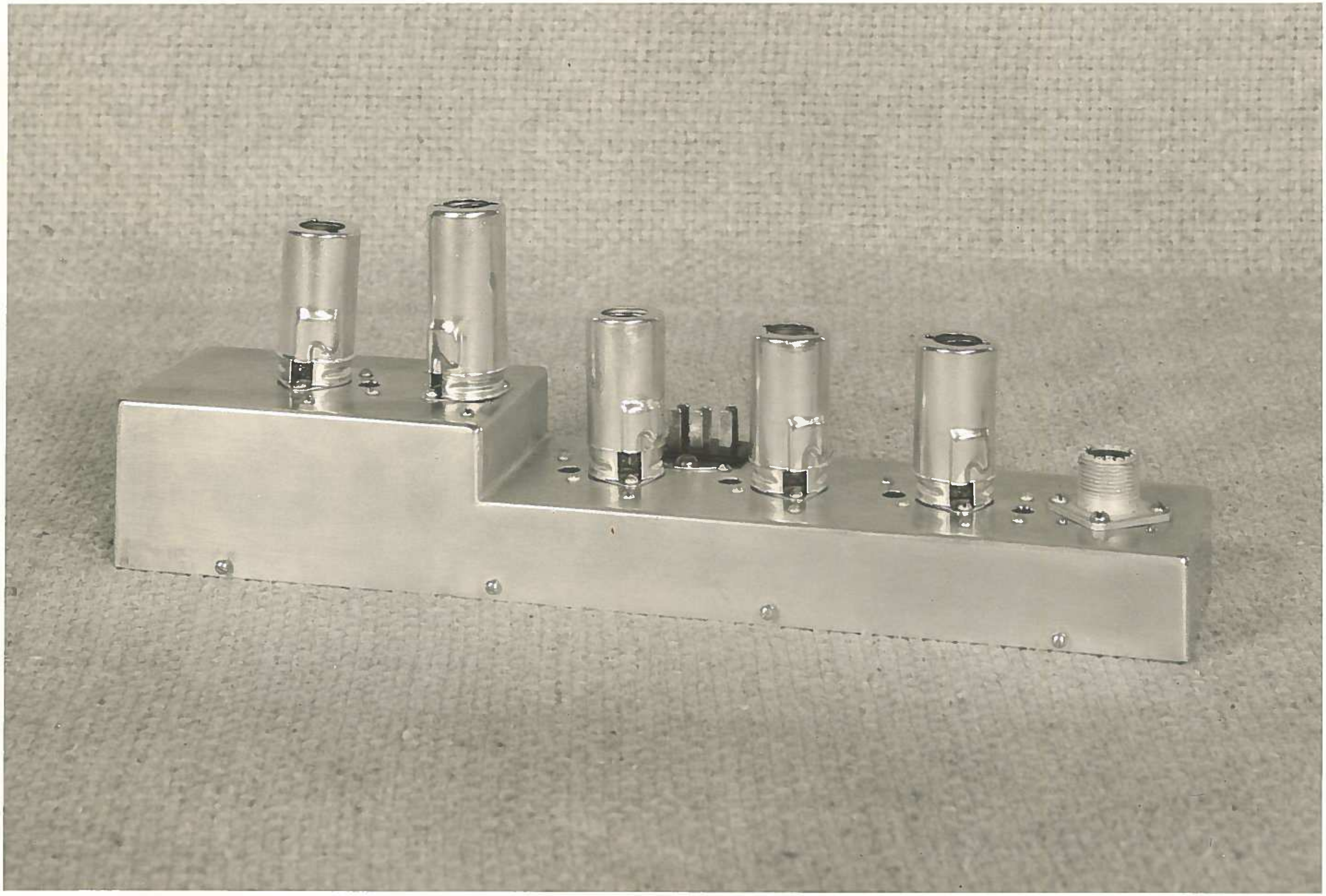

FIG. 12
I-F PREAMPLIFIER USING CASCODE INPUT CIRCUIT
EXTERNAL VIEW

SECRET

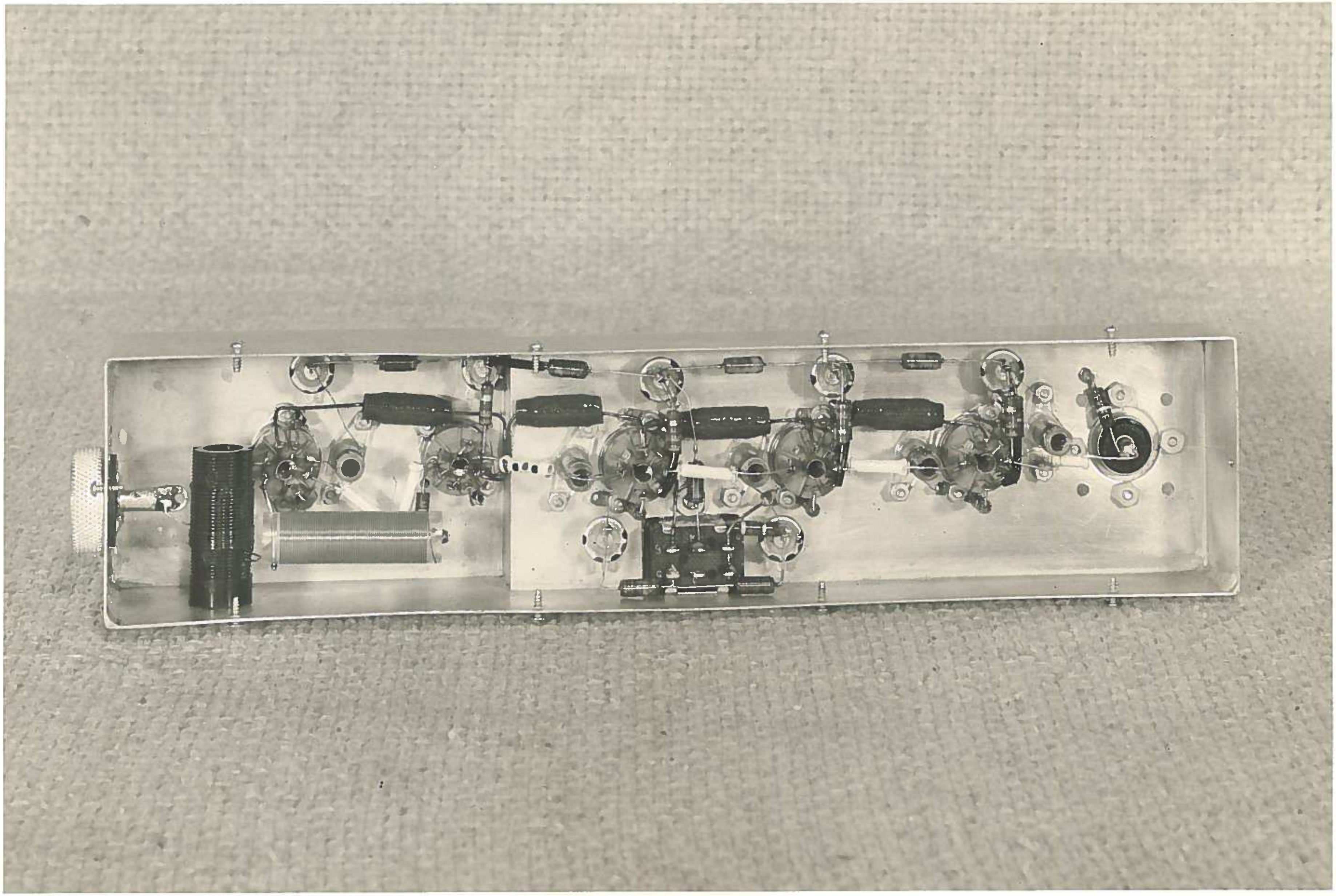

FIG. 13
I-F PREAMPLIFIER USING CASCODE INPUT CIRCUIT
INTERNAL VIEW

SECRET

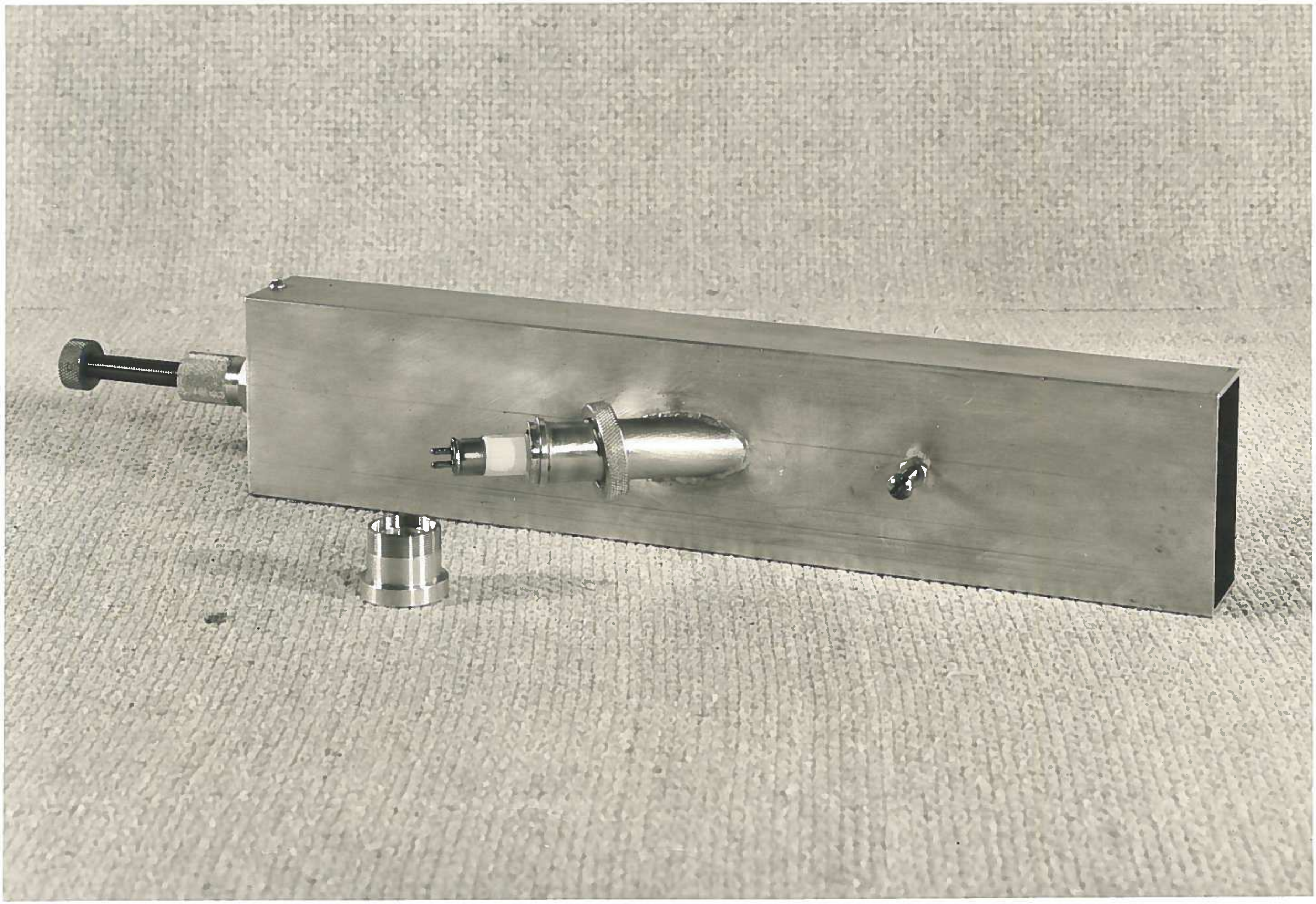

FIG. 14
FLUORESCENT LAMP NOISE GENERATOR

SECRET

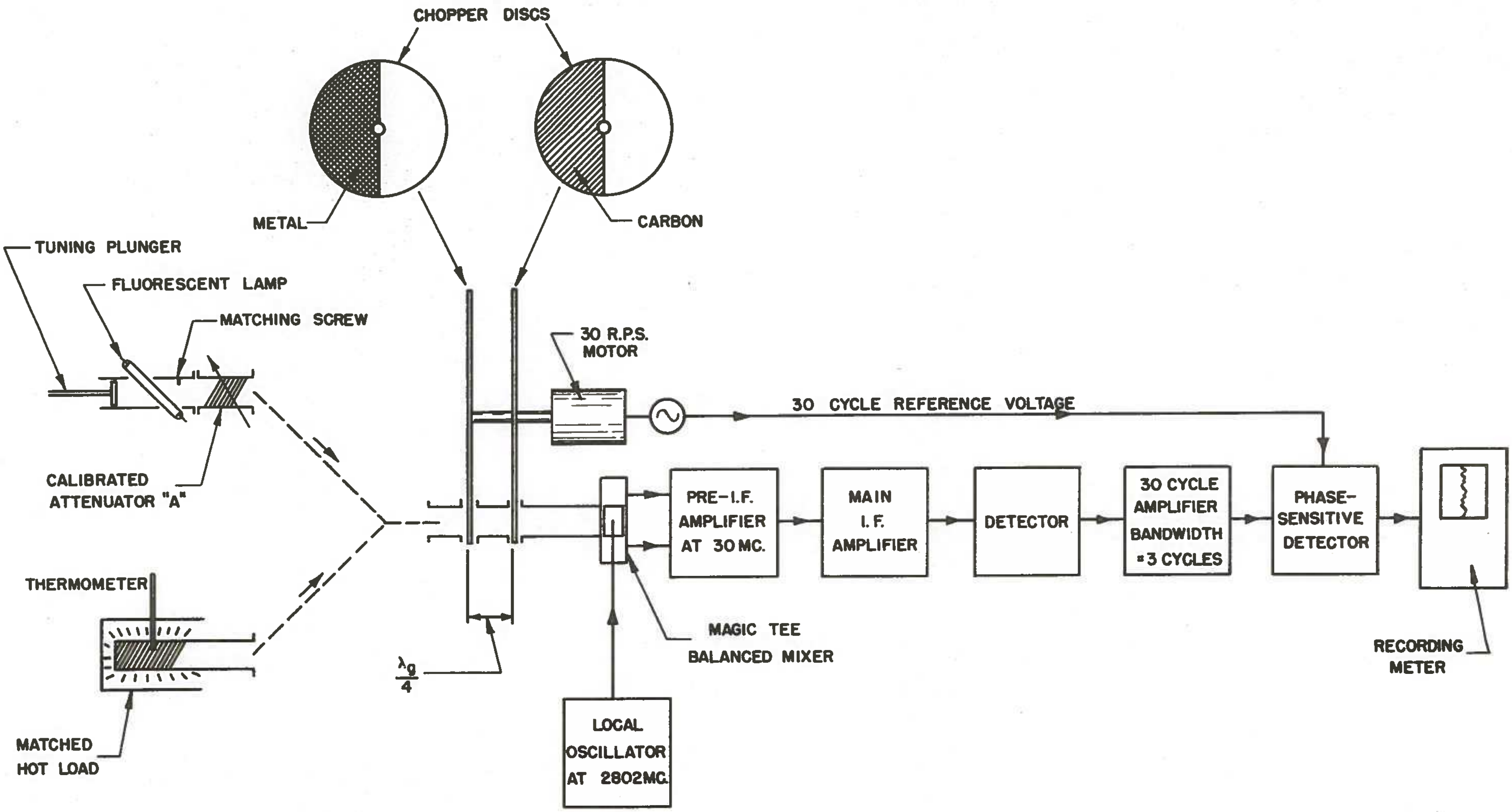

SOLAR NOISE RADIOMETER ADAPTED FOR CALIBRATING NOISE OUTPUT OF FLUORESCENT LAMPS

FIG. 15

To perform the calibration, the heat load is connected to the radiometer input, and a convenient deflection obtained on the recording meter. The fluorescent lamp noise source is substituted, and the matched attenuator A is adjusted until the same deflection is obtained.

Then, E (lamp) = E (heat load) + A (in decibels) Eq. (4)

where $E_{\text{heat load}} = 10 \log_{10}(\frac{T_h}{T_o} - 1)$,

and T_h = absolute temperature of the heat load.

Eq. (4) is discussed in Appendix II.

Mumford's value for excess noise power ratio of the lamp, for a wave-guide temperature of 32°C, was 15.83 decibels, while our results at a wave-guide temperature of 29°C ranged from 15.75 to 15.90 decibels, with an average of 15.84 decibels.

Applying Mumford's temperature correction of -0.055 decibel/°C, our average became 15.68 decibels.

Having thus determined that we had a 3000-megacycle noise source accurate to 0.25 decibel, further radar noise factor readings were made using this lamp as a source.

14. Technique of Measurement Using a Fluorescent Lamp Noise Source

The technique is identical with that used with a noise diode at lower frequencies. The image correction must not be overlooked, however.

A block diagram of the apparatus is shown in Fig.16. The local oscillator, T/R and anti-T/R are adjusted using the signal generator as a source. The second detector current, I, is noted, with the lamp and signal generator off, the padding attenuator in, and the 3-decibel attenuator out of the circuit. The lamp is then switched on, the pad removed, and the 3-decibel attenuator inserted. A is adjusted to duplicate the previous value of I. Then the radar noise factor is determined easily:

Noise Factor = $E_L - A + 10 \log_{10} n$, Eq. (5)

where n is the image correction.

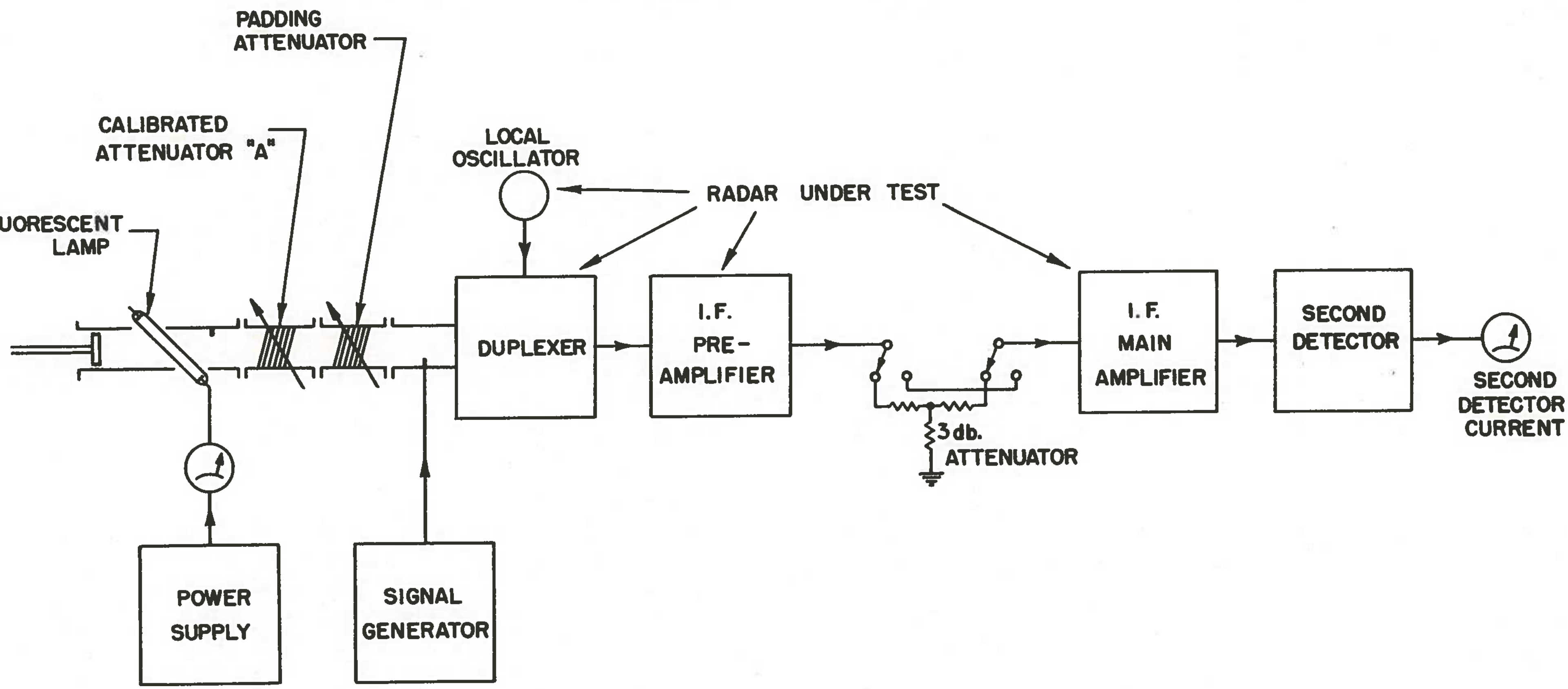

MEASUREMENT OF NOISE FACTOR BY
FLUORESCENT LAMP METHOD

FIG. 16

Eq. (5) is derived in Appendix III, while the image correction is discussed in Appendix I.

15. Comparison with Previous Readings

The noise factors of the Type 980 Receiver and MZPI were remeasured using the fluorescent lamp. Results for a group of crystals are indicated in Fig. 17 and Fig. 19. Satisfactory agreement with the signal generator method was obtained.

16. Tests Using New Preamplifier

The MZPI noise factor was remeasured for various crystals with the new preamplifier in use. The results are plotted in Fig.18. It can be seen that an improvement of 3.6 decibels has been obtained, and also that a further improvement of about 0.6 decibel can now be obtained by rejecting 50 per cent of the crystals. Also indicated in Figs. 17 and 18 is the range of predicted values from Tables I and II. The general agreement here confirms the belief that a further significant improvement cannot be obtained with existing crystals, regardless of mixer design, or type of local oscillator.

17. Image Correction

The over-all frequency response of the Type 980 Receiver was measured. Mechanical integration of the curve indicated that the image correction was 1.3 decibels. This has been added to the noise factors plotted in Fig.19.

A similar measurement on the MZPI indicated an image correction of 0.01 decibel, which is negligible. The difference between the two values is mainly due to the higher intermediate frequency of the MZPI.

18. Crystal Current

The optimum crystal current to be used for best performance is a compromise between conversion loss (g) which improves with increasing crystal current, and noise temperature ratio (t) which deteriorates with increasing crystal current. The use of the new preamplifier with a lower noise factor increases the importance of the second factor (t), resulting in a lower optimum crystal current.

Fig. 20 indicates typical variation in "g" with crystal current*, while Fig. 21 shows "t" versus crystal current. Using these curves and Eq. (3), the variation in noise factor can be predicted as a function

* These measurements were made by W.J. Medd of the Solar Noise Group, N.R.C.

NOISE FACTOR. USING FLUORESCENT LAMP METHOD

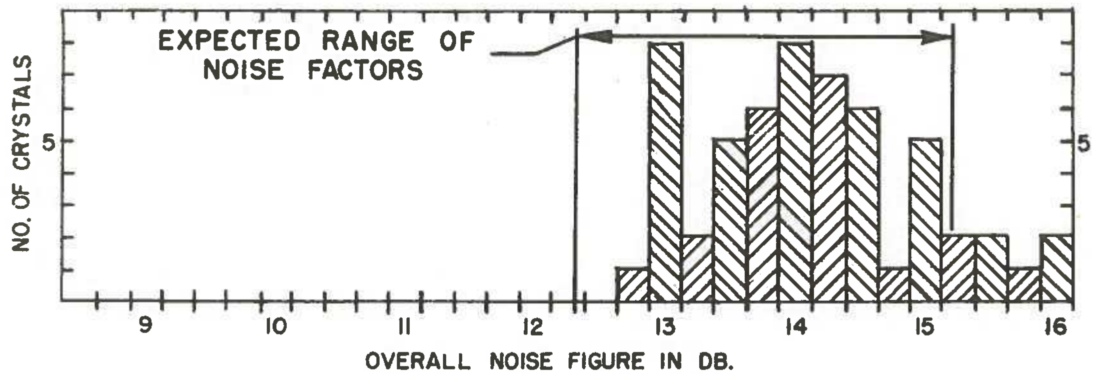

FIG. 17 — MZPI-EXISTING PREAMPLIFIER (VARIOUS IN2IB CRYSTALS)

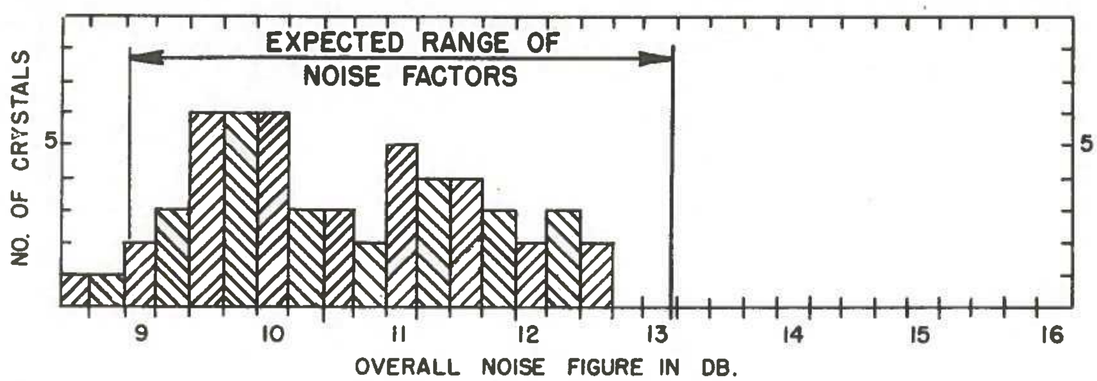

FIG. 18 — MZPI-CASCODE PREAMPLIFIER (VARIOUS IN2IB CRYSTALS)

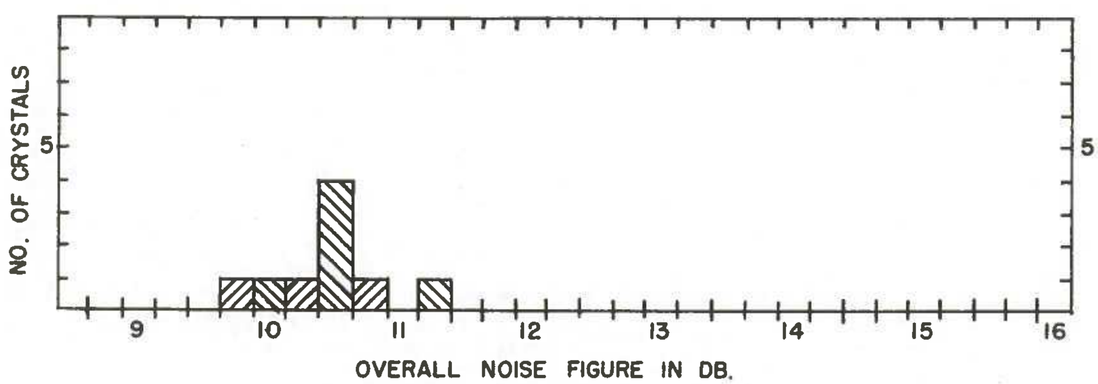

FIG. 19 — 980 RECEIVER (VARIOUS CV364 CRYSTALS)

EFFECT OF CRYSTAL CURRENT ON CRYSTAL PARAMETERS - TYPICAL CRYSTAL

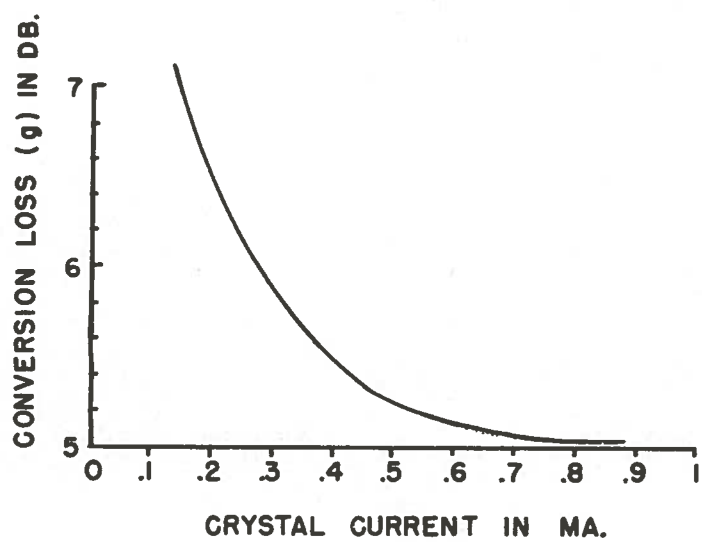

FIG. 20

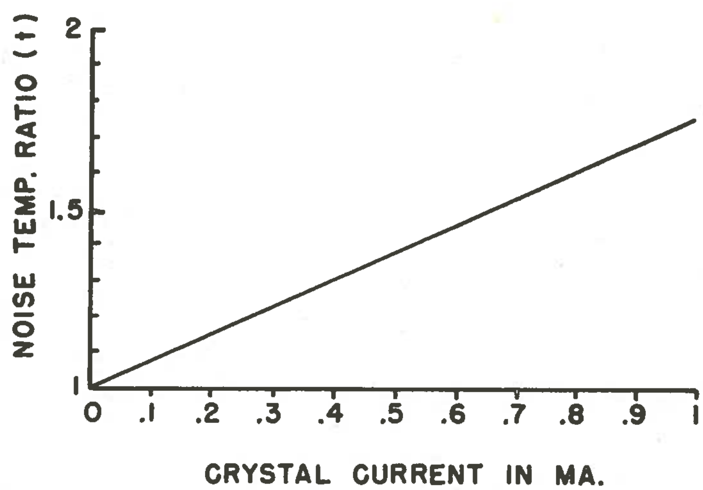

FIG. 21

SECRET

NOISE FACTOR VS. CRYSTAL CURRENT FOR ORIGINAL PREAMPLIFIER

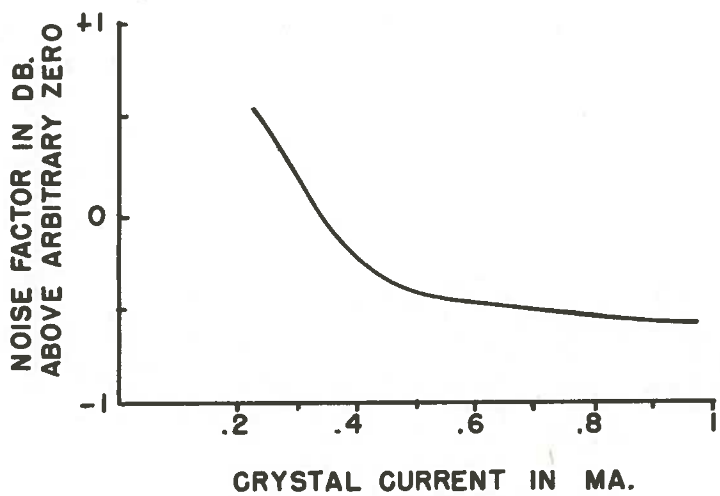

FIG.- 22 CALCULATED FOR TYPICAL CRYSTAL

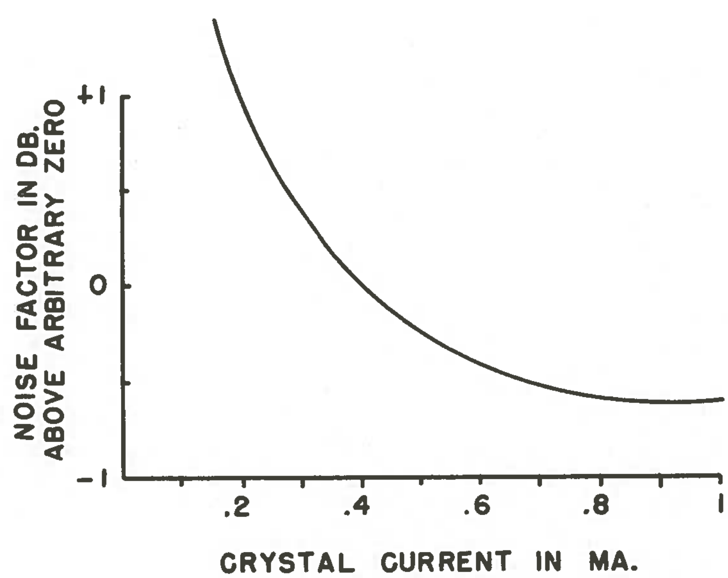

FIG.- 23 OBSERVED - ONE CRYSTAL

NOISE FACTOR VS. CRYSTAL CURRENT FOR CASCODE PREAMPLIFIER

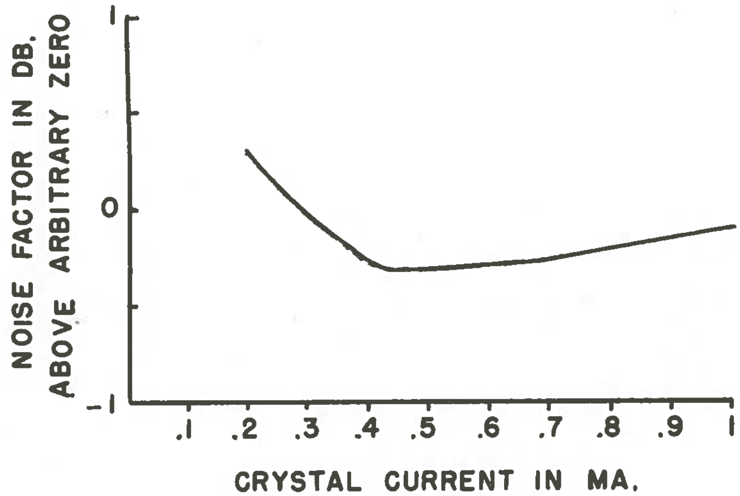

FIG.-24 CALCULATED FOR TYPICAL CRYSTAL

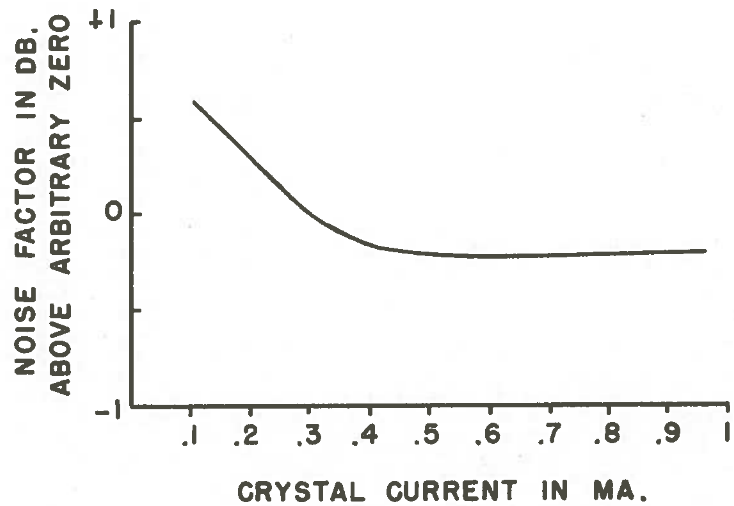

FIG.-25 OBSERVED-ONE CRYSTAL

of crystal current. This has been plotted in Fig.22 for the original preamplifier, and Fig.24 for the cascode preamplifier. A more precise calculation would include the effect of variation in crystal intermediate-frequency impedance with crystal current on the intermediate-frequency noise factor. For design and test of the intermediate-frequency preamplifier, a value of 390 ohms was assumed. This is typical for 1N21B's at 0.5 milliamperes.

Figs. 23 and 25 are experimentally determined relations. It can be concluded that optimum crystal current for the original MZPI is about 0.8 milliamperes, while about 0.5 milliamperes is best if the new preamplifier is used.

19. Choice of Crystal Type

The current price of crystals is about as follows:

1N21B (War Surplus)	$ 0.90 each
1N21B (New)	$ 4.50 each
1N21C (New)	$32.00 each

In view of the difference in price it would be more practical to buy the 1N21B crystals and select the best fifty per cent for use in the signal mixer, than to buy the 1N21C's. This conclusion might not remain valid in future if the characteristics of crystals sold as 1N21B and 1N21C should change.

20. Conclusions

The use of a more up-to-date preamplifier can improve the MZPI noise factor by about 3.6 decibels, which will improve the range on targets above the radar horizon by about 23 per cent. A further range improvement of about 3 per cent can be obtained by rejecting 50 per cent of the crystals. It should be noted that the 3 per cent improvement is too small to be observed in field trials.

It is very doubtful if any changes to the mixer, local oscillator or intermediate frequency would produce a justifiable improvement. It appears that improvement in range should be sought through the use of increased power*, higher total radio-frequency energy per pulse, inclusion of integrating systems**, and optimum use of the magnetron.

* The design of the duplexer for higher power must be carefully worked out in order that the few decibels improvement due to the higher power are not counteracted by an adverse effect on receiver performance due to increased T/R leakage, or other difficulties associated with the ground pulse. Reference (13) is particularly relevant to this matter.

** A concise discussion of integrating systems is given in Reference (11), page 12. Some integration is obtained in the phosphor of the cathode-ray tube screen. Any improvement in phosphors would result in better performance with no increase in complexity of the radar in the field.

(A necessary but not sufficient condition for optimum use of the magnetron is that the tube be used at the limits of its pulse and average power ratings. The term "limit of its pulse rating" implies that no other combination of peak power, pulse width or pulse repetition frequency would give more radio-frequency energy in one pulse.) The use of two alternative pulse widths could be considered.

At the same time it is urgent to follow up the development of two new 3,000-megacycle triodes: the Philips Tube (14), and the General Electric Type L-29. (The Philips tube employs a Lemmens cathode and appears to be the better of the two.)

If first reports of the Philips tube are confirmed, crystal mixers for 3,000-megacycle radars without radio-frequency amplification, will soon be, or may now be, obsolete.

REFERENCES

1. Draft copy of British Admiralty Type 980 Receiver Handbook (N.R.C. Radio Document Control Office Reference No.20644).

2. Dahl and Harper, "An S-band Pre-tuned Mixer", A.S.E. Report XRC2/45/31 (N.R.C. Radio Document Office Reference No.20645).

3. H. Dahl, "A Pre-tuned Frequency Changer for the 10-cm Region", J.I.E.E., Part IIIA, Vol. 93, No.1, p.280.

4. W.J. Kessler, "Effective and Circuit Bandwidths", Electrical Engineering, 1949, p.590.

5. W.R. Bennett, "Response of a Linear Rectifier to Signal and Noise", Bell System Tech. Jour., Vol.23, p.97 (1944).

6. "Crystal Rectifiers", M.I.T. Rad. Lab. Series No. 15, p.32 (McGraw-Hill).

7. M.T. Lebenbaum, "Design Factors in Low Noise Input Circuits", Proc. I.R.E., Jan.,1950, p.75.

8. Wallman, et al, "A Low-noise Amplifier", Proc. I.R.E., June,1948, p.700.

9. "Microwave Receivers", M.I.T. Rad. Lab. Series, No.23, p.321.

10. W.W. Mumford, "A Broad-band Microwave Noise Source", Bell System Tech. Jour., p.608, Oct.,1949.

11. L.A. Moxon, "Recent Advances in Radio Receivers", Cambridge University Press, 1949.

12. D.O. North, "Discussion on Noise Figures of Radio Receivers", Proc. I.R.E., p.125, Feb.,1945.

13. Houlding and Marks, "Deterioration of Crystal Mixer Performance due to T/R Cell Leakage", T.R.E. Tech. Note 66 (N.R.C. Radio Document Control Office Reference No.20765).

14. G. Diemer and K.S. Knol, "Low-level Triode Amplifier for Microwaves", Philips Res. Reports, April,1950, p.153.

APPENDIX I

EFFECT OF IMAGE RESPONSE ON NOISE FACTOR MEASUREMENTS

An alternative definition for noise factor to the one given in Section 4 follows:

The noise factor of a linear receiver (including antenna) is the noise-to-signal power ratio at the output, divided by the noise-to-signal power ratio of an ideal receiver. The characteristics of the ideal receiver are:

1. It contains no sources of noise.

2. It has the same gain at each frequency in the useful channel as the actual receiver, but has zero gain at other frequencies. (The necessity for permitting gain in the useful channel only was pointed out by North[12] and others.)

The frequency response of a typical radar receiver is indicated in Fig.26, while that of the equivalent ideal receiver is given in Fig.27. To measure noise factor N_o, (the available output noise power with no input) is first determined, using arbitrary units. Next a known signal is introduced at the input. We define:

S_I = available excess* power of the test signal (at f_o if a c-w source is used)

OR

P_I = available excess* power per cycle of bandwidth of the test signal (at all frequencies for the case of a noise source).

S_I (or P_I) is varied until S_o (or P_o) = N_o Eq. (6)

(Since there is no way of eliminating N_o the above condition is met by adjusting S_o (or P_o) so that $N_o + S_o$, or $N_o + P_o = 2N_o$.)

To relate S_I and S_o we write:

$$S_o = g_o S_I, \qquad \text{Eq. (7)}$$

* "excess" implies: in addition to thermal noise at room temperature.

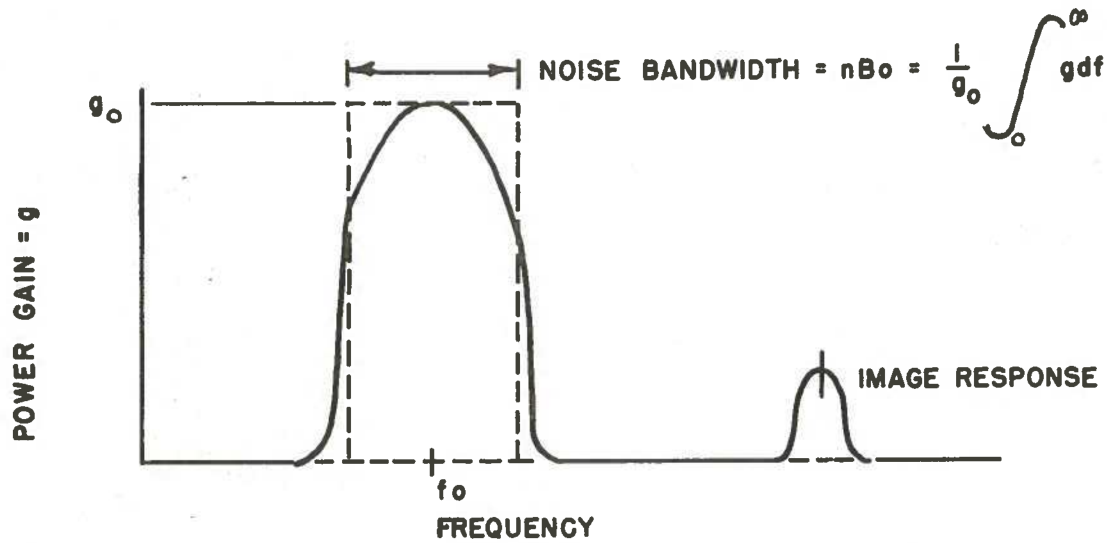

FIG. 26 — TYPICAL RADAR FREQUENCY RESPONSE

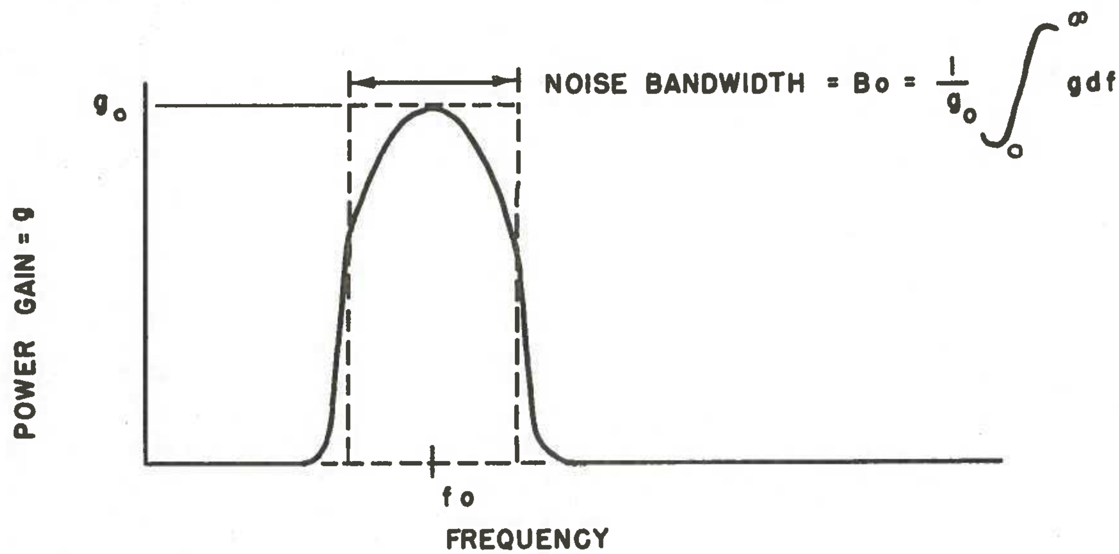

FIG. 27 — EQUIVALENT RESPONSE OF IDEAL RECEIVER

while, if a noise source is used,

$$dP_o = g\ P_I\ df$$

$$P_o = P_I \int_o^\infty g\ df$$

$$= P_I\ g_o\ B_o\ n. \qquad \text{Eq. (8)}$$

Now, the definition of noise factor can be written:

$$F = \frac{\text{Noise power out}}{\text{Noise power out in ideal case}} = \frac{N_o}{N_I} \qquad \text{Eq. (9)}$$

We combine Eqs. (6) and (9) to eliminate N_o:

$$S_o = F\ N_I,$$

or, similarly, $P_o = F\ N_I$.

We introduce Eq. (7) or Eq. (8) to eliminate S_o or P_o,

$$g_o\ S_I = F\ N_I \qquad \text{Eq.(10a)}$$

$$\text{and } g_o\ P_I\ B_o = F\ N_I. \qquad \text{Eq.(10b)}$$

Now, N_I is the output noise from an ideal receiver,

thus, $d\ N_I = g\ K\ T_o\ df$,

$$N_I = KT_o \int_o^\infty g\ df = K\ T_o\ g_o\ B_o.$$

Substituting this value in Eqs.(10a) and (10b):

$$F = \frac{S_I}{K\ T_o B_o}, \qquad \text{Eq. (2)}$$

$$F = n\frac{P_I}{K\ T_o}. \qquad \text{Eq. (2a)}$$

Eqs. (2) and (2a) are used to interpret noise factor measurements using a c-w signal source or a noise source respectively.

It is seen from Eqs. (2) and (2a) that when using a c-w signal, a knowledge of the receiver bandwidth (excluding the image response) is required, while, if using a noise source, the image correction "n" must be known.

APPENDIX II

CALIBRATION OF FLUORESCENT LAMP

By definition of T_L the available noise power from the lamp is $K\ T_L \triangle f$, while by the conditions of the experiment (see Fig. 15), the available noise power from the lamp and attenuator combination is equal to the available noise power from the heat load, which equals $K\ T_H \triangle f$.

Consider now the available noise power from the lamp and attenuator combination. Regardless of the value of the attenuator, there will be at least $K\ T_o \triangle f$ available from the output terminals of the attenuator, as this is the value of its own thermal noise.

The available power from the lamp can be written as follows:

$$P_L = K\ T_L \triangle f = K\ T_o \triangle f + K\ (T_L - T_o)\ \triangle f.$$

The first term on the right-hand side represents noise power in equilibrium with the attenuator at room temperature and is also available at the attenuator output, while the second term (excess noise power) is reduced by a factor "a", where "a" is the attenuation of the attenuator expressed as a power ratio less than one.

Thus,

$$P_A = K\ T_o \triangle f + a\ K\ (T_L - T_o) \triangle f. \qquad \text{Eq.(11)}$$

Hence,

$$T_H = T_o + a\ (T_L - T_o)\ ,$$

$$\left(\frac{T_H}{T_o} - 1\right) = a\ \left(\frac{T_L}{T_o} - 1\right),$$

$$10\ \log_{10}\left(\frac{T_H}{T_o} - 1\right) = 10\ \log_{10}\ a + 10\ \log_{10}\ \left(\frac{T_L}{T_o} - 1\right),$$

$$E_H\ (\text{in db.}) = A\ (\text{in db.}) + E_L\ (\text{in db.}). \qquad \text{Eq. (4)}$$

In the foregoing equations,

T_L = equivalent noise temperature of the fluorescent lamp

K = Boltzmann's constant = 1.38×10^{-23} Joules/°K

T = absolute temperature (degrees Kelvin)

Δf = bandwidth of the radiometer (in cycles per second)

T_H = absolute temperature of heat load

P_L = available noise power from the fluorescent lamp in a bandwidth of Δf.

T_o = 292°K $\doteq$ room temperature

a = attenuation of attenuator (A) as a power ratio

P_A = available noise power from the lamp plus attenuator

E_H = excess noise temperature ratio of heat load

E_L = excess noise temperature ratio of lamp.

APPENDIX III

DERIVATION OF EQUATION (5)

From Eq. (11), the available power from the lamp plus attenuator is

$$P_A = K\,T_o\,\Delta f + a\,K\,(T_L - T_o)\,\Delta f. \qquad \text{Eq.(11)}$$

Now, the excess available power is the second term only, and equals $a\,K\,(T_L - T_o)\,\Delta f$. This quantity per cycle we have defined as P_I (see Appendix I).

Thus,

$$P_I = a\,K\,(T_L - T_o) \qquad \text{Eq.(12)}$$

Eliminating P_I between Eqs. (12) and (2a), we have

$$F = a\,n\,\left(\frac{T_L}{T_o} - 1\right),$$

or

$$10 \log_{10} F = 10 \log_{10} a + 10 \log_{10} n + 10 \log_{10} \left(\frac{T_L}{T_o} - 1\right).$$

$$\text{Noise factor (in db)} = E_L \text{ (in db)} - A + 10 \log_{10} n, \qquad \text{Eq. (5)}$$

where $-A = 10 \log_{10} a$.